

TSF0004

## Experimental Investigation of Water Flow Movement Induced by Ultrasonic Waves

Guillermo Ferrer Sabater<sup>1</sup>, Rafael Royo<sup>1</sup> and Weerachai Chaiworapuek<sup>2,\*</sup>

<sup>1</sup> Escola Tècnica Superior d'Enginyers Industrials (ETSII), Universitat Politècnica de València, Camino de Vera, s/n, 46022 València, Spain

<sup>2</sup> Department of Mechanical Engineering, Faculty of Engineering, Kasetsart University, 50 Ngamwongwan Road, Ladyao, Chatuchak, Bangkok 10900, Thailand

\* Corresponding Author: fengwcc@ku.ac.th, 00-66-2797-0999#1868, 0-2579-4576

### Abstract

The aim of this study is to investigate the characteristics of water movement when it is subjected by high frequency waves. The experiment was carried out in a water tank, having a size of 1m width x 1m length x 0.5 m height. During the test, the water level was kept at 0.3m height. The ultrasonic waves having a frequency of 25 and 40 kHz were generated using the 60 W transducers at a side wall. Data acquisition-processing by hot wire anemometer is utilized to capture the behavior of water flow/particles under the influence of the ultrasonic waves. The obtained results from this experiment were found to reveal the physics of water flow/particles, affected by ultrasound and will be an important information in the field of fluid mechanics.

**Keywords:** Water flow, Ultrasonic waves, Hot wire anemometer, velocity measurement.

### 1. Introduction

Sound waves are found to be the fluctuating pressure, propagating through the medium [1]. They can be classified as shown in Fig.1:

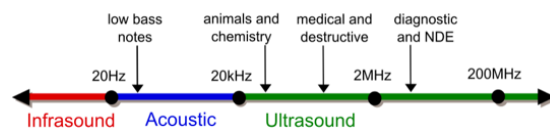


Fig. 1 shows the working range of sound waves

Ultrasounds are sound waves with frequencies higher than the upper audible limit of human hearing, which are between 20 Hz to 20 kHz [2]. Ultrasound is not different from normal (audible) sound in its physical properties, except in that humans can't hear it. Ultrasound devices operate with frequencies from 20 kHz up to several gigahertz. Propagation of sound in a fluid depends mainly on the fluid density, temperature, viscosity, compressibility and elasticity [3]. Sound perturbations produced in a point of an elastic environment propagate through it with a velocity,  $c$ . It can be determined following [3] as:

$$c = 1 / (\rho k)^{0.5} \quad (1)$$

where  $\rho$  = water density (kg/m<sup>3</sup>)  
 $k$  = volumetric compressibility (Pa<sup>-1</sup>)

Temperature has an important influence on the viscosity. The higher temperature, the lower viscosity,

increasing the velocity of wave propagation. In water, as the temperature increases, elasticity will be also increased. Then, this causes the increasing of the wave speed through the medium. Thus, the sound speed in the water at the temperature between 0-100 °C can be yielded from Eq. 1 as shown in Fig.2 :

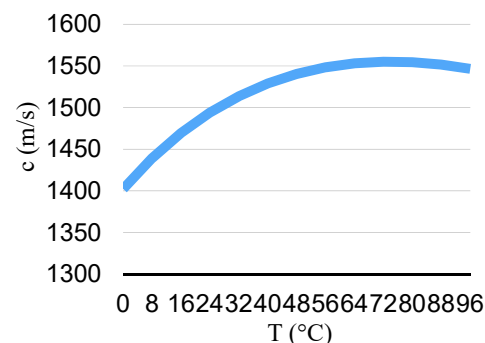


Fig. 2 shows the sound speed in the water

## 2. Ultrasounds generation and acoustic field

To generate ultrasonic waves, piezoelectric materials are usually used by applying the voltages to them. These materials will convert the electric power to mechanical pressure via the vibration. According to the Huygens' principle, the surface transducer is considered as a set of discreted elements, radiating each of hemispherical waves. All elements move synchronously and with equal amplitudes. Consequently, the ultrasonic field produced by a linear array of elements, is concentrated in a more uniform beam when the distance to the transducer is increased. The beam is the region where the waves are in phase. If the emitted beam doesn't have its focal point, it gradually diverges as it passes through the mediums. However, the beam profile can be modified by focusing techniques. The acoustic field from a transducer can be divided into two areas, which are the near and the far fields. The near field is the region, locating next to the transducer or between the transducer and the far field. The near field, also called Fresnel zone, is characterized by a highly collimated beam with large variation in intensity between a wavefront and the next one. It has a distance,  $N$  as shown in Fig.3. Thus, the far field is the area beyond the distance  $N$  where the sound field pressure gradually drops to zero. The far field, also called *distal field* or *Fraunhofer*, is characterized by beam divergence and more uniform intensity between wavefronts.

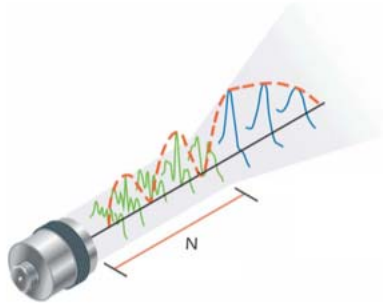


Fig. 3 shows the near and far acoustic fields

Near field distance depends on the frequency of the transducer, its diameter, and the speed of sound in the test material as shown in the following equation (Eq.2):

$$N = D^2 f / 4c \quad (2)$$

Where  $N$  = near field distance (m)  
 $D$  = diameter of the element (m)  
 $f$  = sound frequency (Hz)

The beam spread and the average angle are parameters used to characterize a transducer. Typically, all transducers have a beam spread. Fig. 4 gives a

simplified view of a sound beam for a flat transducer. In the near field, the beam has a complex shape and its diameter decreases along the beam direction. The fluctuating velocity near the source was relatively high comparing to those at the farther distance [4]. Meanwhile, the beam of the far acoustic field diverges at the farther distance from the transducer.

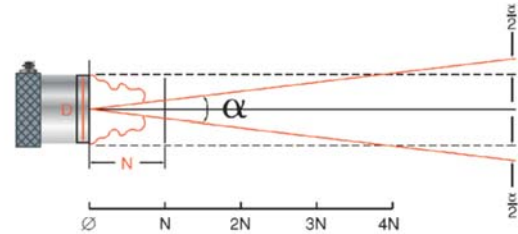


Fig. 4 shows the beam profile of acoustic fields

## 3. Experimental setup

Fig. 5 shows a schematic diagram of the experiment. A water tank, having the size of 1m width x 1m length x 0.5 m height was fabricated by the steel plates that have the thickness of 1 cm. All surfaces of the tank were coated by an anti-rust painting to resist the degradation from the water. The water level was always kept at 0.3 m height through the experiment. An ultrasonic transducer was mounted on a thin stainless steel plate having the thickness of 1 mm. This transducer was made from a piezoelectric ceramic so it can generate the vibration, having the frequency following the obtained input signal. An epoxy glue was used to make a strong bond between the transducer and the thin plate. The 1-mm stainless steel plate was directly installed on a side plate of the test section and the position of the transducer was 20 cm from the bottom plate. With the difference between the thickness of the tank and thin plate, a source of vibration was assumed to occur only from the plate. The frequency and power of vibration, generated from the transducer was controlled by a digital ultrasonic generator. In this study, the velocity of the water flow induced by the ultrasound was measured using a hot film sensor. The vertical location of the sensor was adjustable using a stepping motor. The signal from this probe was transferred to a mini constant temperature anemometer (CTA) box. The CTA signal is a continuous analogue voltage. In order to process it digitally, it has to be sampled as a time series consisting of discrete values digitized by an analogue-to-digital converter (A/D board) and save as data-series in a computer.

The accuracy of the velocity measurement was gained by the method of temperature correction. The temperature, used in this method must be collected by a thermocouple probe, locating near the hot film sensor. With this setup, the velocity was measured correctly even the water temperature changed. Moreover, a

**AECXXX** (this number will be assigned after full manuscript is accepted)

ground probe must be installed in the water tank in order to prevent the destruction of the hot film probe.

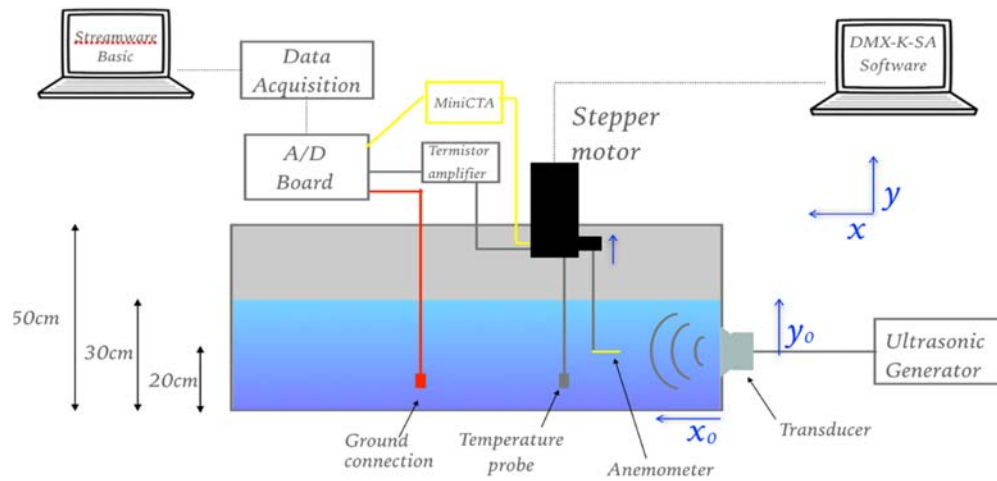


Fig. 5 shows schematic diagram of the experimental setup

In this experiment, the steady state velocity was measured at 4 distances of 2.5 cm, 5 cm, 7.5 cm, and 10 cm from the transducer in x axis using the hot film sensor. In y axis, the measurement started at the middle of the transducer or  $y = 0$  cm from the bottom. It ends at  $y = 8$  cm with the interval of 2.5 mm using the step motor. At each measuring point, the velocity signals were recorded for 6 s after the ultrasonic waves were generated for 10 minutes to obtain the information under steady state condition. The frequency of the ultrasonic waves are set at 25 and 40 kHz. Thus, the obtained results from this study will be presented as the mean and rms velocity signals. Following [5], the magnitude of velocity can be calculated from:

$$U = (1/n) \sum U_i \quad (3)$$

where  $U$  = mean velocity (m/s)  
 $n$  = sampling number  
 $U_i$  = fluctuating velocity signal (m/s)

Meanwhile, the rms velocity can be evaluated as:

$$U_{rms} = [(1/(n-1)) \sum (U_i - U)^2]^{0.5} \quad (4)$$

where  $U_{rms}$  = root mean square velocity (m/s)

#### 4. Results and discussions

From Eqn. 1, the sound speed is 1474.42 m/s where the volumetric compressibility of water is  $4.6 \times 10^{-10}$  1/Pa. Also, from Eqn. 2, the distance of the near acoustic field from the transducer is 0.021 m and 0.033 m for the frequency of 25 kHz and 40 kHz, respectively. Thus, most measurements in this study are in the far field, having uniform velocity profile. Fig. 6 shows the

velocity distribution at  $x = 2.5, 5, 7.5,$  and  $10$  cm and  $y = 0 - 8$  cm with the interval of 2.5 mm under the influence of 25 kHz waves. It should be noted that the wave velocity is normalized using the maximum magnitude in order to compare with those achieved from other positions as:

$$u = U / U_{max} \quad (5)$$

where  $u$  = normalized velocity  
 $U_{max}$  = maximum velocity (m/s)

The results show that, at  $x = 2.5$  cm, the magnitude of velocity during  $y = 0 - 3$  cm is more than those at  $y = 3 - 8$  cm. It means that the velocity magnitude in heightwise direction at the central location of the transducer is more than the other values. The values increase at the farther x, especially at  $y = 7.5 - 17.5$  mm. This clearly presents the characteristic of the wave beam, generated by the transducer. However, the magnitude of the velocity decreases at  $x = 10$  cm. Unlike the distribution of the 25 kHz waves, the maximum velocity of 40 kHz wave is found at  $x = 2.5$  cm and  $y = 2.5$  mm as shown in Fig. 7. The size of the beam increases in radial direction at  $x = 5$  cm. In the mean time, the velocity value decreases at  $x = 7.5$  and  $10$  cm.

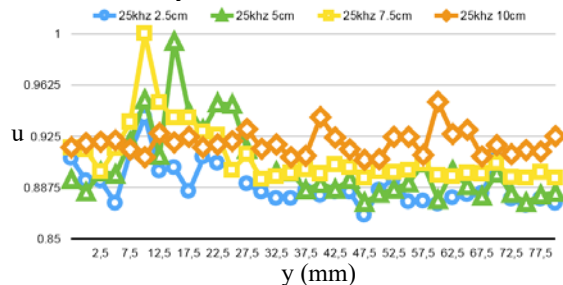


Fig. 6 shows the velocity distribution induced by the 25 kHz waves

**AECXXX** (this number will be assigned after full manuscript is accepted)

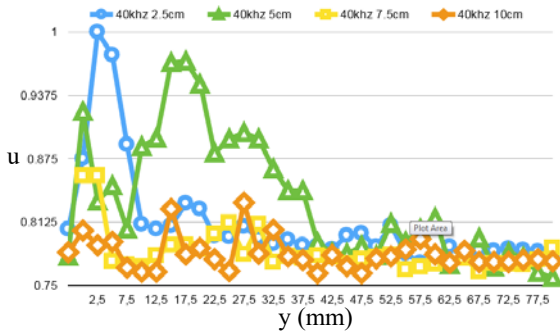


Fig. 7 shows the velocity distribution induced by the 40 kHz waves

Fig. 8 shows the rms velocity distribution at  $x = 2.5, 5, 7.5,$  and  $10$  cm and  $y = 0 - 8$  cm with the interval of  $2.5$  mm under the influence of  $25$  kHz waves. The rms velocity in the figure is also divided by its maximum rms value in order to compare with those yielded from other positions as:

$$u_{rms} = U / U_{rms,max} \quad (6)$$

where  $u_{rms}$  = normalized rms velocity  
 $U_{rms,max}$  = maximum rms velocity (m/s)

The figure shows that the trend of rms velocity corresponds to the trend of mean velocity and the results obtained by [4]. The maximum rms velocity increases along the  $x$ -axis during  $x = 2.5$  to  $7.5$  cm and  $y = 7.5 - 12.5$  mm. However, it is noted that the magnitude of the mean velocity and rms velocity decrease at the central location of the transducer or  $y = 0 - 5$  mm. When the  $40$  kHz waves were applied to the test section, the maximum rms velocity is found at  $x = 5$  cm and  $y = 10$  mm as depicted in Fig.9. The value clearly decreases during  $x = 7.5 - 10$  cm, consistent to the trend of the mean velocity.

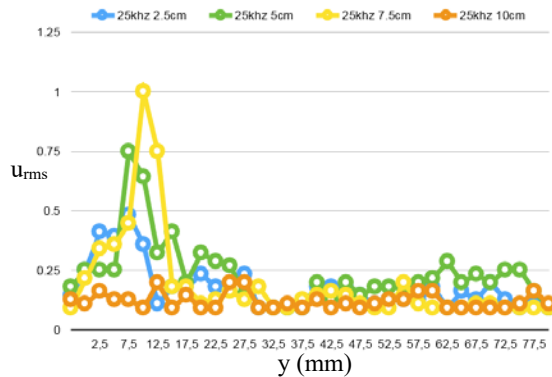


Fig. 8 shows the rms velocity distribution induced by the 25 kHz waves

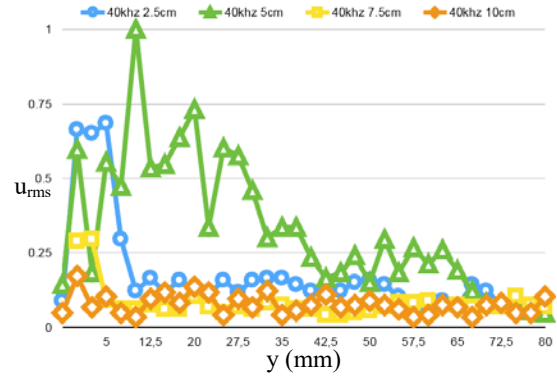


Fig. 9 shows the rms velocity distribution induced by the 40 kHz waves

The mean velocity distribution of the water at  $x = 2.5$  cm induced by the  $25$  and  $40$  kHz is compared as shown in Fig. 10. The figure reveals that the magnitude of water velocity under the influence of  $40$  kHz waves is more than those obtained from  $25$  kHz condition. At this position, the peak of the signal is found at  $y = 5$  mm under the  $40$  kHz waves while it disappears under the  $25$  kHz waves. These trend manner was consistent to those of the fluctuating velocity as shown in Fig. 11. From the figure, the high difference is found around the peak or  $y = 0 - 10$  mm. In the mean time, the other values of  $u_{rms}$  between the case of  $25$  and  $40$  kHz at  $y > 10$  mm is in the same level.

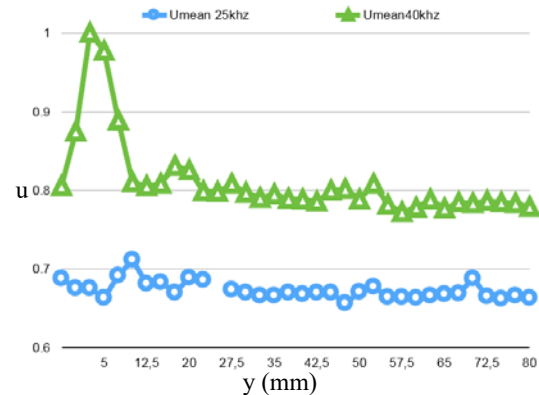


Fig. 10 shows the comparison between the water velocity induced by the  $25$  kHz and  $40$  kHz waves at  $x = 2.5$  cm

**AECXXX** (this number will be assigned after full manuscript is accepted)

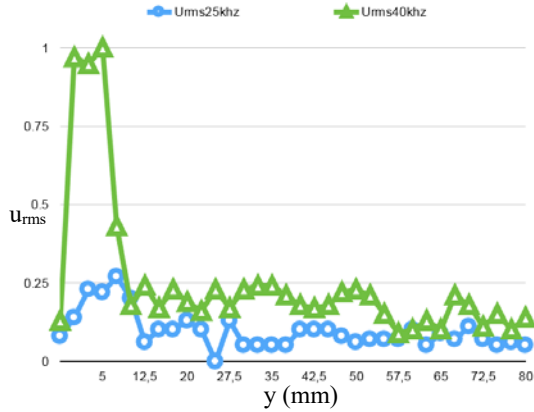


Fig. 11 shows the comparison between the rms velocity induced by the 25 kHz and 40 kHz waves at  $x = 2.5$  cm

At the distance of  $x = 5$  cm from the transducer, the water velocity induced by the 40 kHz is more than those under the influence of 25 kHz waves as depicted in Fig. 12. Unlike those yielded at  $x = 2.5$  cm, the difference of the  $u_{rms}$  between 25 and 40 kHz can be found between  $y = 0 - 65$  mm as shown in Fig. 13.

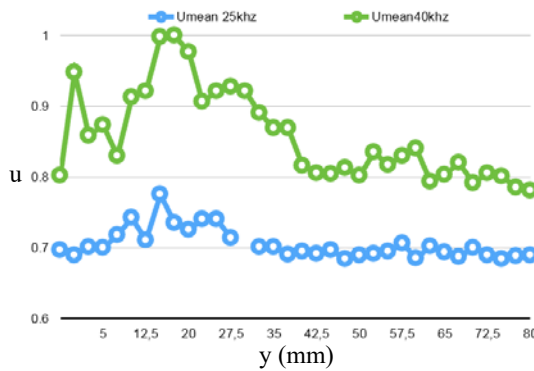


Fig. 12 shows the comparison between the water velocity induced by the 25 kHz and 40 kHz waves at  $x = 5$  cm

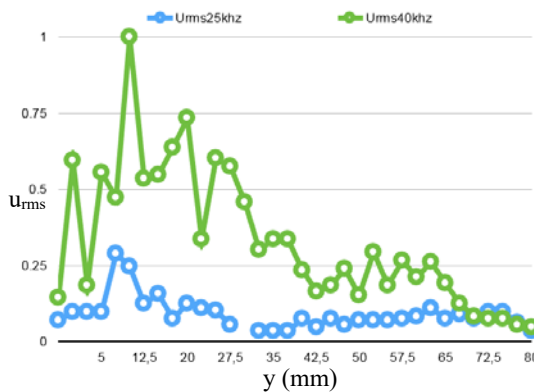


Fig. 13 shows the comparison between the rms velocity induced by the 25 kHz and 40 kHz waves at  $x = 5$  cm

Fig. 14 shows the comparison between the water velocity induced by the 25 kHz and 40 kHz waves at  $x = 7.5$  cm. The results show that the peak of each case appears at different  $y$  position and their value is not much different as those achieved at  $x = 2.5$  and 5 cm. The maximum  $u_{rms}$  of the flow under the 25 kHz is close to the value of maximum  $u_{rms}$  in the case of 40 kHz as illustrated in Fig. 15. Meanwhile, the values measured during  $y = 15 - 80$  mm become not different again at this location.

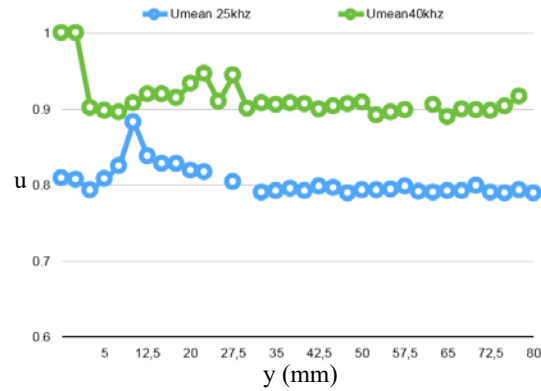


Fig. 14 shows the comparison between the water velocity induced by the 25 kHz and 40 kHz waves at  $x = 7.5$  cm

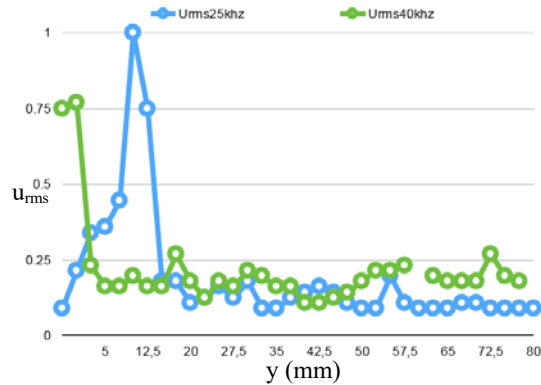


Fig. 15 shows the comparison between the rms velocity induced by the 25 kHz and 40 kHz waves at  $x = 7.5$  cm

At  $x = 10$  cm from the ultrasonic transducer, the peak of the  $U$  signal measured from the water flow under the 25 and 40 kHz waves can not be found as depicted in Fig. 16. This behavior is also found from the  $u_{rms}$  signals as shown in Fig. 17. From this figure, the results show that the  $u_{rms}$  yielded from the water induced by the 25 kHz waves is much less than those from the flow under the 40 kHz ultrasonic waves. The values are found to be near zero.

AECXXX (this number will be assigned after full manuscript is accepted)

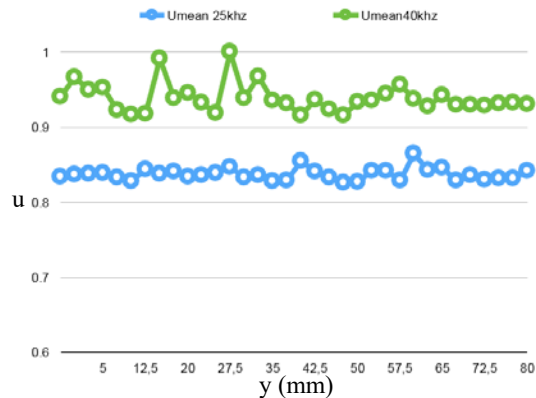


Fig. 16 shows the comparison between the water velocity induced by the 25 kHz and 40 kHz waves at  $x = 10$  cm

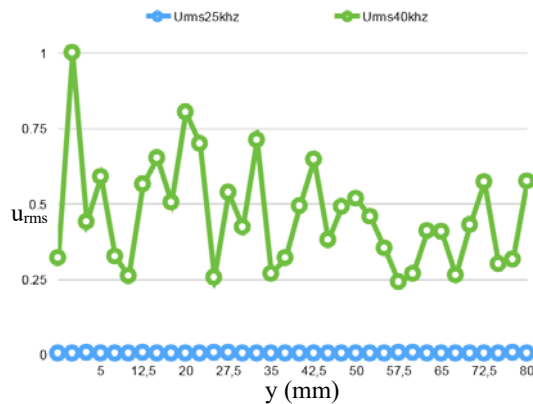


Fig. 17 shows the comparison between the rms velocity induced by the 25 kHz and 40 kHz waves at  $x = 10$  cm

### 5. Conclusions

In this study, the mean and rms velocities of water induced by the 25 and 40 kHz ultrasonic waves were measured in a water tank using the hot film sensor. The results show that the ultrasound induces an acoustic streaming in the water tank. The beam characteristics are found near the central location of the transducer. The maximum magnitude is found during  $x = 5 - 7.5$  cm and  $x = 2.5 - 5$  cm when the water is under the influence of 25 and 40 kHz ultrasonic waves, respectively. Also, these results are in agreement with the trend of rms velocity distribution. Moreover, it is found that the 40 kHz vibration from the ultrasonic transducer can generate the faster and more fluctuating waves comparing with those obtained from the 25 kHz transducer.

### 6. Acknowledgement

The authors gratefully acknowledge the financial support from Faculty of Engineering, Kasetsart University, Thailand.

### 7. References

- [1] Cheeke, J.D.N. (2002). Fundamentals and Applications of Ultrasonic Waves, CRC Press, New York, USA.
- [2] Legay, M., Gondrexon, N., Le Person, S., Boldo, P., and Bontemps, A. (2011). Enhancement of Heat Transfer by Ultrasound: Review and Recent Advances, *International Journal of Chemical Engineering*, vol. 2011, pp. 1 - 17.
- [3] Dunkhin, A.S., and Goetz, P.J. (2008). Ultrasound for Characterizing Colloids, Elsevier, Netherlands.
- [4] Kumar, Ajay, Kumaresan, T., Pandit, A.B., and Joshi, J.B. (2006). Characterization of low phenomena induced by ultrasonic horn, *Chemical Engineering Science*, vol. 61, pp. 7410-7420.
- [5] Munson, B.R., Young, D.F., and Okiishi, T.H. (2006). Fundamental of Fluid Mechanics, 5th Ed. John Wiley & Sons, USA.